

Improving distribution system state estimation with synthetic measurements

Jose M. Cano^{a,*}, Pablo Arboleya^a, Mahmoud Rashad Ahmed^a, Md Rejwanur R. Mojumdar^b, Gonzalo A. Orcajo^a

^a Department of Electrical Engineering, University of Oviedo, 33204 Gijón, Asturias, Spain

^b Department of Energy and Petroleum Engineering, University of Stavanger, 4036 Stavanger, Norway

ARTICLE INFO

Keywords:

Advanced metering infrastructure
Distribution system state estimation
Synthetic measurements

ABSTRACT

Distribution state estimation is a desired feature of modern power systems. The availability of measurements from smart meters has opened the door to extend the application of state estimation techniques down to end customers, preferably at the secondary distribution transformer level. However, the light coupling between phases makes the estimation of certain state variables, such as voltage phase angles, a great challenge. This paper proposes the use of synthetic measurements as a means of including cross-coupled information in the available set of measurements. This possibility can be easily implemented in line supervisors located at secondary transformer stations without the need for new hardware, just by embracing a different connection of measurement devices. This work demonstrates that this costless action results in a strong reduction of the sensibility of phase angle estimation errors with respect to measurement noise, thus leading to an important improvement in the quality of the results.

1. Introduction

The recent deployment of advanced metering infrastructure (AMI) throughout the distribution system, including low voltage (LV) networks, have triggered the interest of utilities in tools to monitor this traditionally blind spot of the grid. Thus, state estimation (SE) algorithms, which have been ubiquitous in transmission systems since the 70s, are now being adapted to the specific characteristics of these networks.

Important challenges had been pointed out by researchers working on the application of distribution system state estimation (DSSE), apart from the imperative need to deal with unbalance conditions or the well-known reduced redundancy of measurements which characterizes this part of the system. Indeed, the size of the problem makes it essential to use a hierarchical structure, which implies distributed tools at the sub-station level [1,2]. Moreover, the availability of heterogeneous measurements from different sources, such as SCADA or smart meters, calls for algorithms capable of dealing with different time scales [3]. Furthermore, some of these data cannot be obtained in a synchronous way, forcing the use of time-dependent measurement weights and

pseudo-measurements [4]. Aside from these challenges, the present work deals with a poorly studied issue which characterizes 4-wire systems at the end-user level: the difficulty of estimating voltage phase angles in an environment of very light coupling between phases [5]. The use of a set of synthetic measurements is proposed in this contribution as an efficient way of obliterating this important problem.

In Section 2, the typical measurement infrastructure used by European utilities is described. A regular structure of a DSSE algorithm is outlined in Section 3. Section 4 introduces synthetic measurements as a means of improving the quality of the estimation. The benefits of the proposal are clearly highlighted in two case studies presented in Section 5. Finally, the conclusions of this work are drawn in Section 6.

2. Typical setup of measurement infrastructure

Data gathered from smart meters enable the possibility of conducting an SE at the distribution transformer level. Indeed, voltage and active and reactive power measurements from each customer can be reported by these devices under request. Nonetheless, the availability of these measurements is not so obvious as, depending on the communication

* Corresponding author.

E-mail addresses: jmcano@uniovi.es (J.M. Cano), arboleyapablo@uniovi.es (P. Arboleya), UO278851@uniovi.es (M. Rashad Ahmed), md.r.mojumdar@uis.no (M.R.R. Mojumdar), gonzalo@uniovi.es (G. A. Orcajo).

<https://doi.org/10.1016/j.ijepes.2020.106751>

Received 17 June 2020; Received in revised form 18 December 2020; Accepted 21 December 2020

Available online 15 February 2021

0142-0615/© 2021 The Author(s). Published by Elsevier Ltd. This is an open access article under the CC BY license (<http://creativecommons.org/licenses/by/4.0/>).

type, delays can have a serious impact on the quality of the SE. This work does not try to contribute to this important issue, but to handle the problem of lack of coupling between the different phases. The latter concern can seriously deteriorate the quality of the estimation even if a simultaneous snapshot of the measurements is available.

Fig. 1 shows an example of the measurement infrastructure used by a European utility. Both single-phase and three-phase smart meter units, rely on phase-to-neutral voltages to comply with their measurement tasks. Thus, phase-to-neutral voltages and per-phase active and reactive power are available under request, being the preferred values used to feed the SE algorithm. Smart metering data concentrator units (DCU), among other tasks, can play the role of routers between the smart meters at the end customer locations and the energy management system (EMS) of the utility, regardless of the distributed or centralized nature of the latter. However, other important set of measurements is used by utilities in order to foster the accuracy of the results and increase the observability of the problem. A transformer station supervisor (TSS) and sometimes line supervisors (LSs), are deployed at the secondary side of distribution transformers with the aim of monitoring phase-to-neutral voltages, line currents, and active and reactive power flowing into the LV side. Traditionally, TSSs and LSs are used by the utility to monitor transformer load, detect problems in voltage regulation, identify faulty phases, and make rough power balances which can help in fraud detection. Data from those supervisors can be added to the measurement set of the SE algorithm, thus taking advantage of the existing infrastructure. In the case of the example shown in Fig. 1, data from the TSS and LSs are obtained by the EMS through the LV remote terminal unit (RTU); however, different hardware layouts can be observed in different utilities.

3. DSSE algorithm

A standard implementation of the WLS augmented matrix 4-wire SE algorithm is used in this contribution to illustrate the potential benefits of synthetic measurements. According to the augmented matrix approach [6], the following set of linearized equations describes the SE problem

$$\begin{bmatrix} \alpha^{-1}R & H & 0 \\ H^T & 0 & C^T \\ 0 & C & 0 \end{bmatrix} \begin{bmatrix} \mu_s \\ x^{k+1} - x^k \\ \lambda_s \end{bmatrix} = \begin{bmatrix} z - h(x^k) \\ 0 \\ -c(x^k) \end{bmatrix}, \quad (1)$$

where,

- the leftmost term is the so-called Hachtel's matrix,
- x is the vector of state variables (SVs),

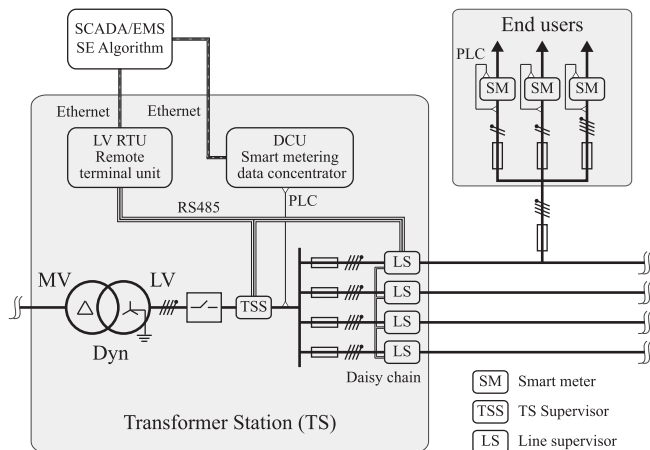


Fig. 1. An example of modern measuring infrastructure in a distribution transformer station.

- z is the vector of regular measurements,
- h is the vector of non-linear functions relating regular measurements to state variables,
- c is the vector of non-linear functions relating virtual measurements (typically equaling zero) to state variables,
- R is the measurement error covariance matrix, with variances of regular measurement errors at its diagonal,
- H is the Jacobian of regular measurements,
- C is the Jacobian of virtual measurements,
- α is a scale factor used to improve the condition number of the Hachtel's matrix with no influence on the estimated state (it is selected in this work as the minimum variance of the set of regular measurement errors),
- μ_s is the vector of scaled Lagrange multipliers for regular measurements,
- λ_s is the vector of scaled Lagrange multipliers for virtual measurements,
- k stands for the iteration order.

Phase-to-ground voltage magnitudes, $V_{i,p}$, and phase angles, $\theta_{i,p}$, at each bus, i , and phase, $p \in \{abc\}$, and at the neutral conductor, $V_{i,n}$ and $\theta_{i,n}$, are taken as state variables, i.e. $x = [\theta|V]^T$, with V and θ being the vectors gathering those variables.

The set of regular measurements, z , and their corresponding measurement functions (h -functions), consist of: (1) phase-to-neutral voltage magnitudes from smart meters and TSS or/and LSs, V_z , (2) active and reactive power injections from smart meters, P, Q , and (3), line current magnitudes, I , and active and reactive power flows, P_f, Q_f , from TSS or/and LSs. The measurement functions corresponding to active and reactive power flows are of special interest for this work, and thus, they are explicitly derived in the following with the help of Fig. 2. Consider the admittance $g_{ij,p} + jb_{ij,p}$ of the conductor at phase $p \in \{abc\}$ which directly connects buses i and j . The active and reactive power flowing from bus i to j is directly obtained from the phasors of the measured variables, $v_{zi,p}$ and $i_{ij,p}$, and can be expressed as a function of the SVs as

$$\begin{aligned} P_{f_{ij,p}} &= \text{Re}\{v_{zi,p} \cdot i_{ij,p}^*\} \\ &= g_{ij,p} [V_{i,p}^2 - V_{i,p}V_{j,p}\cos(\theta_{i,p} - \theta_{j,p}) \\ &\quad - V_{i,n}V_{i,p}\cos(\theta_{i,n} - \theta_{i,p}) + V_{i,n}V_{j,p}\cos(\theta_{i,n} - \theta_{j,p})] \\ &\quad + b_{ij,p} [-V_{i,p}V_{j,p}\sin(\theta_{i,p} - \theta_{j,p}) \\ &\quad - V_{i,n}V_{i,p}\sin(\theta_{i,n} - \theta_{i,p}) + V_{i,n}V_{j,p}\sin(\theta_{i,n} - \theta_{j,p})] \end{aligned} \quad (2)$$

$$\begin{aligned} Q_{f_{ij,p}} &= \text{Im}\{v_{zi,p} \cdot i_{ij,p}^*\} \\ &= g_{ij,p} [-V_{i,p}V_{j,p}\sin(\theta_{i,p} - \theta_{j,p}) \\ &\quad - V_{i,n}V_{i,p}\sin(\theta_{i,n} - \theta_{i,p}) + V_{i,n}V_{j,p}\sin(\theta_{i,n} - \theta_{j,p})] \\ &\quad + b_{ij,p} [-V_{i,p}^2 + V_{i,p}V_{j,p}\cos(\theta_{i,p} - \theta_{j,p}) \\ &\quad + V_{i,n}V_{i,p}\cos(\theta_{i,n} - \theta_{i,p}) - V_{i,n}V_{j,p}\cos(\theta_{i,n} - \theta_{j,p})] \end{aligned} \quad (3)$$

The set of virtual measurements, and their corresponding c -

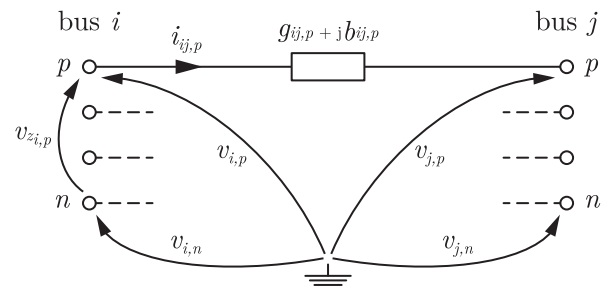


Fig. 2. Calculation of measurement functions for power flows at TSS and LSs from state variables.

functions, consist of: (1) active and reactive power injections at zero-injection buses, which are forced to be equal to zero and (2), the balance of currents at each bus (except for the one at the secondary of the transformer), which is forced to be zero (i.e. the sum of input and output currents, including neutral).

A flat profile is considered during the initialization of the SVs for the iterative process.

4. Introduction of synthetic measurements

Low voltage feeders, especially in residential areas, show a very low coupling between phases. Certainly, single-phase loads are prevalent in this case, and thus, most of the load connections and available measurements, relate one specific phase with the neutral conductor. This fact makes it hard for SE algorithms to provide an accurate estimation of voltage phase angles. Notice that, with the type of measurements described in Section 2, a zero impedance neutral conductor would make these SVs unobservable, as each phase conductor would be, in that case, fully decoupled from the rest of the circuit. Even if that is a non-realistic approach, the truth is that the influence of each phase on the others is very limited and conditioned by the value of the neutral impedance. Thus, even if voltage phase angles are theoretically observable, measurement errors make those SVs hard to be obtained within an acceptable accuracy range, and frequently, can lead to the divergence of DSSE algorithms. Mathematically, an insight into this fact can be obtained from the calculation of the M_{xz} matrix [7], which is used in sensitivity analysis to assess the influence of measurement errors, on SVs, x , at the true state, x^{true} . The M_{xz} matrix can be directly obtained as a part of the inverse of the Hachtel's matrix evaluated at x^{true} , as

$$\begin{bmatrix} \alpha^{-1}R & H & 0 \\ H^T & 0 & C^T \\ 0 & C & 0 \end{bmatrix}^{-1} = \begin{bmatrix} M_{\mu z}[r \times r] & M_{\mu c}[r \times (N+v)] \\ M_{xz}[N \times r] & M_{xc}[N \times (N+v)] \\ M_{\lambda z}[v \times r] & M_{\lambda c}[v \times (N+v)] \end{bmatrix} \cdot \quad (4)$$

M_{xz} is the only term of interest in (4), where the size of the different submatrices have been explicitly shown, N being the number of SVs and r and v the number of regular and virtual measurements, respectively.

Large values in those elements associated with voltage phase angles in M_{xz} are a clear symptom of ill-conditioning of the problem. Considering that one of the phase-to-ground voltage phase angles at the slack bus (which in this case, corresponds to the secondary of the transformer), is taken as a reference by the SE algorithm, large values of the elements of the matrix are expected at any bus on the other two phases and neutral. That is, being phase a the one selected as a reference w.l.o.g. and m each of the available measurements, the subset, g , of SVs, leading to large sensitivities can be represented as

$$M_{xz}(g, m) = \left. \frac{\partial x_g}{\partial z_m} \right|_{x=x^{true}} = \left. \frac{\partial \theta_{i,bcn}}{\partial z_m} \right|_{x=x^{true}}, \quad (5)$$

where θ stands for the voltage phase angle, i for the bus, and b, c and n for the affected phases and neutral.

In this work, the introduction of synthetic measurements is proposed as an efficient and costless tool, capable of removing the aforementioned ill-condition by forcing the coupling between phases. With this aim, the electric connections at the TSS are changed as shown in Fig. 3. In this way, the TSS continues to provide the rms value of line currents, I , but not the per-phase power flows, P_f and Q_f . Instead of that, the cross-coupling between phase-to-neutral voltages and line current probes provides a set of synthetic measurements, P_f^{syn} and Q_f^{syn} . Even if these measurements do not furnish any physical magnitude, they are still valid to be included into the SE algorithm and, more importantly, they provide information with a high coupling between phases. Though other configurations can be also valid, the three single-phase power measurement devices of the TSS in Fig. 3.b are fed with currents, i_a, i_b and i_c from the CTs but with the shifted set of phase-to-neutral voltages v_b, v_c

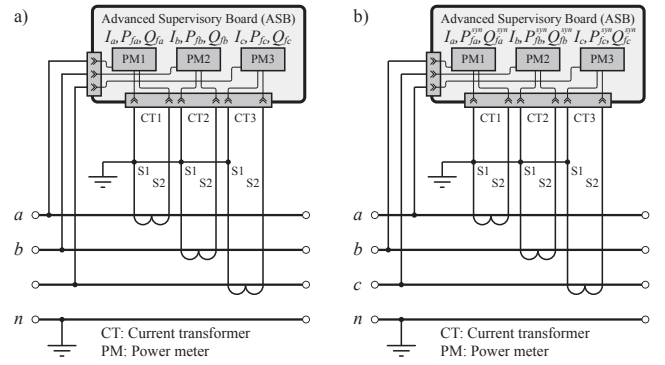


Fig. 3. Connections of the voltage and current transducers to the Advanced Supervisory Board (ASB) used by the TSS. a) Standard setup, and b) Modified setup used to provide coupled information through synthetic measurements.

and v_a , respectively.

Only slight modifications of the WLS augmented matrix 4-wire SE algorithm, previously shown in Section 3, are required to support synthetic measurements. Those changes apply to the measurement functions corresponding to synthetic active and reactive power flow measurements and their related Jacobian terms in the H matrix. According to Fig. 4, if the voltage probe of a power meter which monitors the current at phase p is shifted to a different phase, s , then, the active and reactive power flowing from bus i to j is now obtained from the phasors $v_{z_{i,s}}$ and $i_{j,p}$ of the measured variables, and can thus be expressed as a function of the SVs as

$$\begin{aligned} P_{j,p}^{syn} &= \text{Re}\{v_{z_{i,s}} \cdot i_{j,p}^*\} \\ &= g_{ij,p} [V_{i,s} V_{j,p} \cos(\theta_{i,s} - \theta_{j,p}) \\ &\quad - V_{i,s} V_{j,p} \cos(\theta_{i,s} - \theta_{j,p}) \\ &\quad - V_{i,n} V_{j,p} \cos(\theta_{i,n} - \theta_{j,p}) + V_{i,n} V_{j,p} \cos(\theta_{i,n} - \theta_{j,p})] \\ &\quad + b_{ij,p} [V_{i,s} V_{j,p} \sin(\theta_{i,s} - \theta_{j,p}) \\ &\quad - V_{i,s} V_{j,p} \sin(\theta_{i,s} - \theta_{j,p}) \\ &\quad - V_{i,n} V_{j,p} \sin(\theta_{i,n} - \theta_{j,p}) + V_{i,n} V_{j,p} \sin(\theta_{i,n} - \theta_{j,p})] \end{aligned} \quad (6)$$

$$\begin{aligned} Q_{j,p}^{syn} &= \text{Im}\{v_{z_{i,s}} \cdot i_{j,p}^*\} \\ &= g_{ij,p} [V_{i,s} V_{j,p} \sin(\theta_{i,s} - \theta_{j,p}) \\ &\quad - V_{i,s} V_{j,p} \sin(\theta_{i,s} - \theta_{j,p}) \\ &\quad - V_{i,n} V_{j,p} \sin(\theta_{i,n} - \theta_{j,p}) + V_{i,n} V_{j,p} \sin(\theta_{i,n} - \theta_{j,p})] \\ &\quad + b_{ij,p} [-V_{i,s} V_{j,p} \cos(\theta_{i,s} - \theta_{j,p}) \\ &\quad + V_{i,s} V_{j,p} \cos(\theta_{i,s} - \theta_{j,p}) \\ &\quad + V_{i,n} V_{j,p} \cos(\theta_{i,n} - \theta_{j,p}) - V_{i,n} V_{j,p} \cos(\theta_{i,n} - \theta_{j,p})] \end{aligned} \quad (7)$$

The corresponding terms of the measurement Jacobian, i.e. $dP_f^{syn}/d\theta$, dP_f^{syn}/dV , $dQ_f^{syn}/d\theta$ and dQ_f^{syn}/dV , directly follows from (6) and (7).

Notice that, even if the EMS is now not being directly fed with per-phase power flow measurements, those values can be still available to

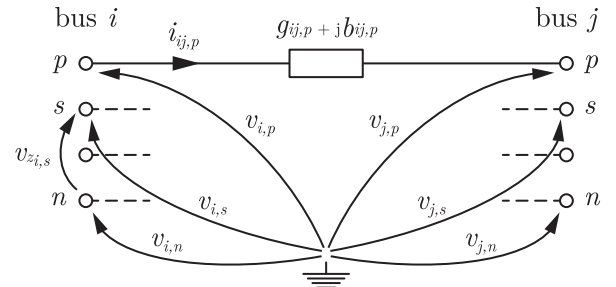


Fig. 4. Calculation of measurement functions for synthetic power flows at TSS and LSs from state variables.

be used by the utility, as they can be obtained as a by-product of the state estimator.

As it is demonstrated in the following section, the inclusion of this set of measurements, providing coupled information between the different phases, drastically reduces the magnitudes of the outliers found in the M_{xz} matrix, specifically those highlighted in (5), thus turning the problem into well-conditioned, and making it possible to obtain accurate estimates of the voltage phase angles.

5. Case studies

5.1. Case Study I: Benchmark circuit

In order to highlight the significant benefits of using synthetic measurements and compare the results with those obtained from a standard measurement setup, an extremely simplified system with 4 buses is considered in this section. Table 1 gathers the data of line impedances, single-phase loads and voltages at the slack bus. The values of the SVs of this circuit, shown in the 3rd and 4th columns of Table 2, are obtained by using a custom made unbalanced power flow (PF) algorithm which results were verified with OpenDSS [8]. Measurements from smart meters and a LS located at Line 1–2 were obtained from the aforementioned solution through the addition of Gaussian noise, except for a set, considered as unavailable, which is specified in Table 1. Following the guidelines provided in [6], the standard deviations used to generate the corrupted measurements are obtained as

$$\sigma = k \cdot \gamma \cdot FS, \tag{8}$$

where FS stands for the full scale of the measurement device, γ for its precision class and k is a number which depends on the type of measurement. The specific values used in this case study are shown in Table 1. A custom made 4-wire WLS state estimator using the augmented matrix concept, as described in Section 3, was used to estimate the SVs of the circuit, both for the standard measurement setup and for the one using synthetic measurements. Table 2 shows the marked improvements in accuracy obtained in the latter case, especially in the estimates of voltage phase angles. In fact, the maximum error, which is found in $\theta_{4,c}$, drops from 3.52 deg. to 1.10 deg., thus achieving a reduction of more than 68%. These improvements can be easily explained by noticing the

Table 1

Data – Case Study I.

		Lines				
From bus	To bus	R_{abc} [pu]	R_n [pu]	X_{abcn} [pu]		
1	2	1.8e-2	2.9e-2	1.7e-3		
2	3	3.2e-2	5.1e-2	3.0e-3		
2	4	2.4e-2	3.8e-2	2.9e-3		
Loads						
Bus	P_{1a} [kW]	P_{1b} [kW]	P_{1c} [kW]	Q_{1a} [kvar]	Q_{1b} [kvar]	Q_{1c} [kvar]
2	10	3	0	1	2	0
3	0	8	8	0	2	2
4	1	3	4	2	2	-3
Slack bus voltages – Secondary of the distribution transformer						
Bus	$V_{1,a}$ [pu]	$V_{1,b}$ [pu]	$V_{1,c}$ [pu]	$\theta_{1,a}$ [deg.]	$\theta_{1,b}$ [deg.]	$\theta_{1,c}$ [deg.]
1	1	0.95	1	0	-123	120
Measurement error parameters						
	Voltages	Power injections	Power flows	Currents		
$k \cdot \gamma$	0.001	0.005	0.005	0.002		
Full scale	350 V	12 kW/kvar	15 kW/kvar	50 A		
Unavailable meas.	$V_{22c}, V_{23a}, V_{23b}$	P_{3b}, Q_{3b}	P_{12b}	I_{12c}		

$$V_{base} = 400/\sqrt{3} \text{ V}; S_{base} = 10 \text{ kVA}$$

Table 2

Comparison of state estimation results.

Bus	Phase	PF Results		SE Standard Set		SE Synthetic Set	
		V [pu]	θ [deg.]	V [pu]	θ [deg.]	V [pu]	θ [deg.]
1	a	1.000	0.00	1.000	0.00	1.000	0.00
	b	0.950	-123.00	0.948	-124.46	0.949	-122.32
	c	1.000	120.00	0.999	116.49	0.999	119.83
	n	0.000	0.00	0.000	0.00	0.000	0.00
2	a	0.980	0.18	0.981	0.18	0.980	0.17
	b	0.919	-122.49	0.917	-123.95	0.918	-121.81
	c	0.981	119.87	0.980	116.35	0.980	119.69
	n	0.028	-149.53	0.027	-152.54	0.028	-148.43
3	a	0.980	0.18	0.981	0.17	0.980	0.17
	b	0.888	-122.30	0.885	-123.73	0.886	-121.61
	c	0.961	120.23	0.960	116.72	0.960	120.06
	n	0.066	-162.97	0.064	-165.46	0.066	-162.10
4	a	0.977	0.43	0.978	0.43	0.977	0.42
	b	0.910	-122.23	0.908	-123.69	0.909	-121.55
	c	0.972	119.39	0.971	115.88	0.971	119.22
	n	0.056	-157.16	0.054	-159.97	0.056	-156.41

significant reduction of the sensitivity of SV estimation errors with respect to measurement errors, which can be verified by analyzing the elements of the M_{xz} matrix. As an example, Fig. 5 shows the sensitivity of $\theta_{4,b}$ with respect to the full set of measurements for both the standard setup and the one including the synthetic set. Errors in voltage measurements are revealed as the main determinant of increased sensitivity in SV errors.

5.2. Case Study II: Real distribution grid

A real European LV distribution grid in the north of Spain, which is depicted in Fig. 6, is considered in this second case study in order to test the validity of the proposal in a high demanding context. The grid has 76 3-phase buses and feeds a total of 54 single-phase dwellings equipped with smart meters. A TSS is used to monitor phase-to-neutral voltages, power flows and currents at the secondary of the transformer. Fig. 6 shows the location of the smart meters, zero-injection buses and TSS. The load profile of the dwellings, sampled every minute during a 24-h period is used by an unbalance PF algorithm to calculate the SVs of the grid. Then, the same procedure of Case Study I is followed: measurements from smart meters and TSS are calculated from the SVs and Gaussian noise is added considering standard deviation values according to (8). For simplicity, all measurements are considered as available in this case study. The topological data of the circuit, load profiles, true state and measurements can be downloaded from [9]. A total of 608 SVs have to be determined at 1440 snapshots in two cases: (1) using traditional measurements, i.e. standard power flow values at the TSS and (2),

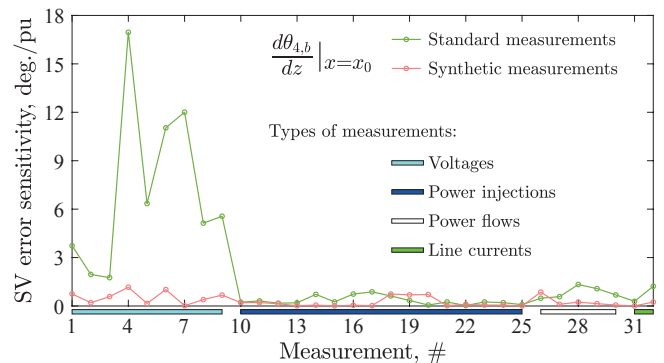


Fig. 5. Sensitivity of $\theta_{4,b}$ with respect to the full set of measurements.

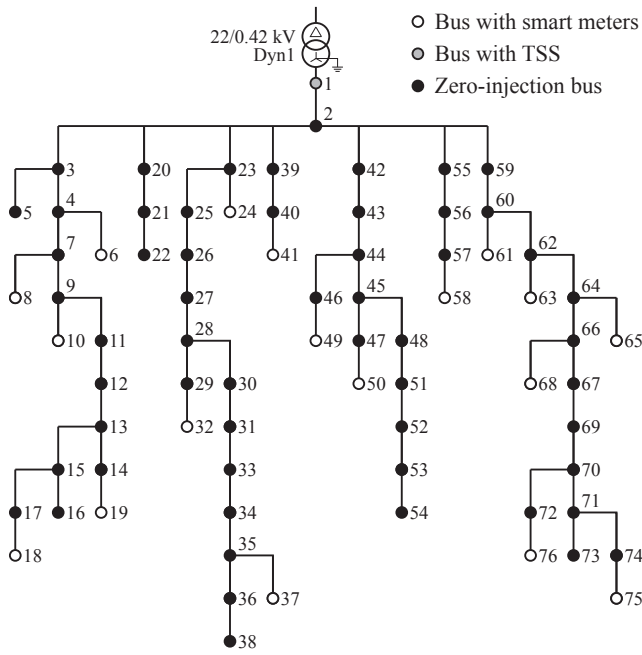


Fig. 6. Layout of a European LV distribution grid in the north of Spain.

using synthetic measurements. The dimension of the problem and the diversity of operating points ensures the statistical relevance of the conducted test.

Table 3 shows the results of the application of the unbalance SE algorithm at one specific instant (the last minute sample of the 24-h period has been considered for this purpose). Four terminal buses, 18, 37, 50 and 75, have been selected to compare the results of the two different estimation strategies. The 3rd and 4th columns of the table show the true state of the system at the selected instant, obtained using a custom made unbalance PF algorithm which results were verified using OpenDSS [8]. The estimation obtained from the standard set of measurements using the SE algorithm described in Section 3 are shown in the 5th and 6th columns of Table 3. The 7th and 8th columns of the table show the estimation obtained using the synthetic set (i.e. synthetic power flows at the TSS), by including the modifications of the SE algorithm highlighted

Table 3
Comparison of state estimation results at terminal buses – last time sample.

Bus	Phase	PF Results		SE Standard Set		SE Synthetic Set	
		V [pu]	θ [deg.]	V [pu]	θ [deg.]	V [pu]	θ [deg.]
18	a	1.048	-0.04	1.047	-0.03	1.048	-0.03
	b	1.048	-120.03	1.048	-115.40	1.048	-119.28
	c	1.048	119.91	1.048	123.25	1.048	120.14
	n	0.002	-15.66	0.002	-20.66	0.002	-18.52
37	a	1.049	-0.02	1.049	-0.02	1.049	-0.02
	b	1.049	-120.04	1.049	-115.40	1.049	-119.29
	c	1.039	120.05	1.039	123.38	1.039	120.27
	n	0.014	97.37	0.014	100.42	0.014	97.77
50	a	1.049	-0.03	1.049	-0.03	1.049	-0.03
	b	1.049	-120.00	1.049	-115.36	1.049	-119.25
	c	1.048	119.91	1.048	123.24	1.048	120.13
	n	0.001	137.93	0.001	149.90	0.001	141.59
75	a	1.047	-0.04	1.047	-0.05	1.047	-0.05
	b	1.046	-120.07	1.047	-115.43	1.047	-119.31
	c	1.036	120.03	1.036	123.37	1.036	120.26
	n	0.014	100.20	0.014	102.69	0.015	100.50

$$V_{base} = 400/\sqrt{3} \text{ V}$$

in Section 4. It can be immediately noticed that, while the estimation of voltage magnitudes provides excellent results in both cases, the estimation of voltage phase angles at phases *b* and *c* show important deviations from the true state of the system. This error is significantly reduced if the synthetic set of measurements is considered. Indeed, from Table 3, it can be concluded that the maximum absolute error of 4.64 deg., which appears at bus 75 phase *b*, is reduced to 0.76 deg. The estimation of voltage phase angles at the neutral conductor is a particularly difficult challenge due to the low values of these voltages; however, their estimation shows also a significant improvement with the proposed strategy, with the maximum error, which takes place at bus 50, being reduced from 11.97 deg. to 3.66 deg.

The sensitivities of two angles at terminal buses, $\theta_{18,b}$ and $\theta_{37,c}$, were obtained at the last time sample from the evaluation of M_{xz} at x^{true} . These sensitivities are shown in Fig. 7 for the full set of measurements, considering both the standard setup and the one including the synthetic set. As in the case of the benchmark circuit, a significant reduction of angle sensitivities is achieved by the use of synthetic measurements. The negative effect of voltage measurement errors is particularly mitigated by the proposed methodology. Although only two specific cases are shown in Fig. 7, the same sensitivity pattern can be observed at any voltage phase angle along the grid (at phases *b* and *c*) for any snapshot.

In order to compare the results of both SE strategies in a wide variety of operating points, the estimations of voltage phase angles at bus 75 have been analyzed during a 24-h period with a sampling time of 1-min. Thus, the histogram of the absolute errors in the estimation of $\theta_{75,b}$ and $\theta_{75,c}$ are presented in Fig. 8 for the case of both the standard and synthetic measurement sets. The average value of these errors in the case of the standard set reaches 4.43 deg. and 3.36 deg. for phases *b* and *c*, respectively. On the contrary, the use of synthetic measurements reduces the average value of the errors to 0.32 deg. and 0.21 deg. Moreover, the maximum absolute errors reach completely unacceptable values in the case of the standard set, with outliers up to 147.59 deg. at phase *b*; however, the use of the synthetic set reduces the maximum error to 2.27 deg. Finally, the 95th percentile of the error distribution, CP95, equals 11.90 deg. and 10.81 for phases *b* and *c*, i.e. 5% of the

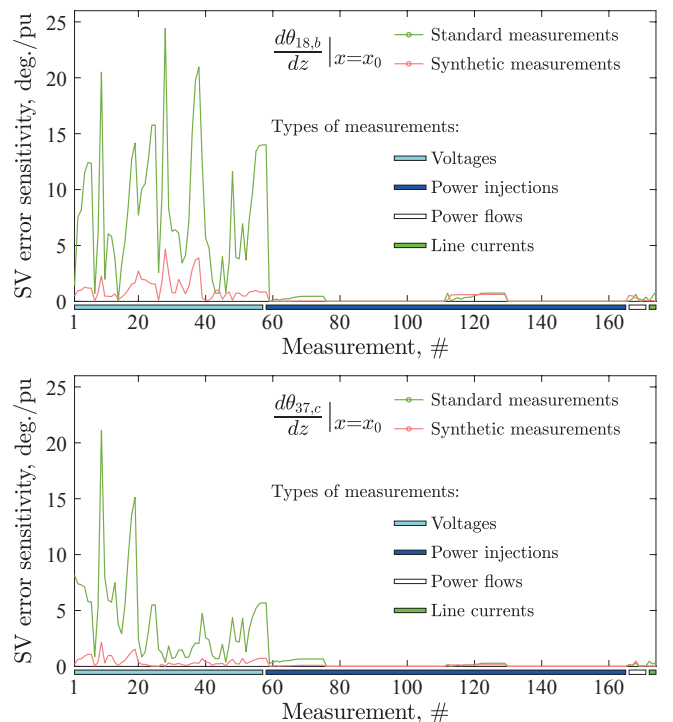


Fig. 7. Sensitivity of $\theta_{18,b}$ and $\theta_{37,c}$ with respect to the full set of measurements at the last time sample.

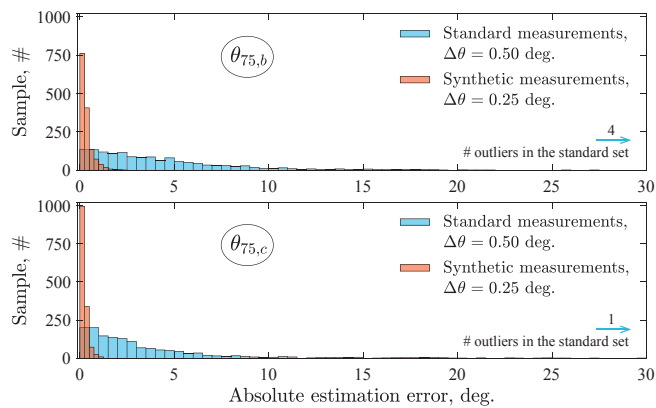


Fig. 8. Histogram of the absolute error of voltage phase angles at bus 75, $\theta_{75,b}$ and $\theta_{75,c}$, for 1440 snapshots corresponding to a 1-min sampling rate during a 24-h period.

operating points under study lead to errors greater than these values. Conversely, the CP95 is reduced in the case of synthetic measurements to 0.96 deg. and 0.58 deg. at phases *b* and *c*, respectively.

6. Conclusion

The light coupling between phases poses a challenge to the application of distribution state estimation techniques at the LV level. Indeed, the use of the standard set of measurements obtained from smart meters and line supervisors, even in the ideal case of being free of delays, can lead to extremely poor estimates of voltage phase angles. Certainly, under this light coupling conditions, the sensitivity of voltage phase angle estimation errors to measurement noise shows large values, which can turn the estimation process into an ill-conditioned problem. This work introduces the use of synthetic measurements as a costless and efficient way of endowing DSSE algorithms with cross-coupled information between phases, thus leading to accurate angle estimates. These so-called synthetic measurements, in the sense that they do not provide physical quantities, can be obtained from line supervisors or transformer station supervisors just with minor changes in the connections of their voltage probes.

Data availability

Datasets related to this article can be found at <https://doi.org/10.17632/2t5pxcr8m4.1>, an open-source online data repository hosted at Mendeley Data [9].

.17632/2t5pxcr8m4.1, an open-source online data repository hosted at Mendeley Data [9].

CRedit authorship contribution statement

Jose M. Cano: Conceptualization, Methodology, Software, Writing - original draft. **Pablo Arboleya:** Formal analysis, Data curation, Validation. **Mahmoud Rashad Ahmed:** Software, Writing - review & editing. **Md Rejwanur R. Mojumdar:** Visualization, Writing - review & editing. **Gonzalo A. Orcajo:** Project administration, Supervision.

Declaration of Competing Interest

The authors declare that they have no known competing financial interests or personal relationships that could have appeared to influence the work reported in this paper.

Acknowledgements

This work was supported by the Spanish Government Innovation Development and Research Office under grant DPI2017-89186-R and the Government of the Principality of Asturias under Grant FC-GRUPIN-IDI/2018/000241.

References

- [1] Gómez-Quiles C, Gómez-Expósito A, de la Villa Jaen A. State estimation for smart distribution substations. *IEEE Trans Smart Grid* 2012;3(2):986–95.
- [2] Pau M, Patti E, Barbierato L, Estebsari A, Pons E, Ponci F, Monti A. Design and accuracy analysis of multilevel state estimation based on smart metering infrastructure. *IEEE Trans Instrum Meas* 2019;68(11):4300–12.
- [3] Gómez-Expósito A, Gómez-Quiles C, Dzafic I. State estimation in two time scales for smart distribution systems. *IEEE Trans Smart Grid* 2015;6(1):421–30.
- [4] Alimardani A, Therrien F, Atanackovic D, Jatskevich J, Vaahedi E. Distribution system state estimation based on nonsynchronized smart meters. *IEEE Trans Smart Grid* 2015;6(6):2919–28.
- [5] Langner AL, Abur A. Role of the reference bus in three-phase state estimation. In: 2019 North American Power Symposium (NAPS); 2019. p. 1–6.
- [6] Abur A, Gómez-Expósito A. *Power system state estimation: theory and implementation*. CRC Press; 2004.
- [7] Caro E, Conejo A, Mínguez R. A sensitivity analysis method to compute the residual covariance matrix. *Electric Power Syst Res* 2011;81(5):1071–8.
- [8] Dugan RC, Montenegro D. *The Open Distribution System Simulator (OpenDSS): Reference guide, program rev. 8.6.1 ed.*, EPRI, June 2019.
- [9] Cano JM, Arboleya P, Ahmed MR, Mojumdar MRR, Orcajo GA. Data for: Improving distribution system state estimation with synthetic measurements, doi: 10.17632/2t5pxcr8m4.1, Mendeley Data, V1; 2020.